Errors resulting from finite beamwidth and sample dimensions in the determination of the ultrasonic absorption coefficient

J. L. Drewniak, L. A. Frizzell, and F. Dunn
Bioacoustics Research Laboratory, University of Illinois, 1406 West Green Street, Urbana, Illinois 61801

(Received 14 November 1989; accepted for publication 26 March 1990)

The error resulting from heat conduction in the measurement of the ultrasonic absorption coefficient using the transient thermoelectric method is studied analytically. An expression for the temperature increase in a tissue specimen of finite dimensions, irradiated by a focused ultrasonic transducer, is given as a function of spatial coordinates, time, radial and axial beam dimensions, and absorption. An error is defined, and results are presented for various values of beamwidth, tissue dimensions, absorption, and time for the purpose of quantifying the experimental error due to heat conduction, and to provide guidance for minimizing this error in experimental procedures. For example, it is shown that the effect of heat conduction on the measured rate of temperature increase is less than 7% when using a transducer with a 5-mm half-power beamwidth at depths greater than 1.5 mm in the tissue.

PACS numbers: 43.35.Yb, 43.80.Ev

INTRODUCTION

It has long been established that physical damage to soft tissues can result from heat deposition upon exposure to ultrasound.[1–3] The acoustic quantity characterizing the conversion of acoustic energy to heat is the absorption coefficient. Knowledge of the absorption coefficient as a function of frequency and temperature, together with known values for the thermal properties of tissue, allows approximate calculations of the temperature increase through use of the bioheat equation and subsequent assessment of thermal risk to the tissue.

Two methods, viz., the transient thermoelectric method (TTM),[4] and the pulse decay method (PDM),[5,6] are currently employed to measure the absorption coefficient α in soft tissue. Both techniques seek to determine the absorption coefficient from[7,8]

$$\rho C_p \frac{\partial T_{nc}}{\partial t} = 2\alpha I = 2\alpha I_0 e^{-2\alpha d}, \qquad (1)$$

where the density ρ, the heat capacity per unit mass C_p, and the intensity I at the tissue depth of interest d are assumed known, and $\partial T_{nc}/\partial t$ is the measured rate of increase of temperature with no heat conduction. The intensity at the site of temperature observation is determined from the free-field intensity I_0 by correcting for attenuation, which is taken here as approximately equal to the absorption.[9] Since the conduction term in the heat equation is zero only when the heat source is uniform and infinite in extent, which is not the case in practice, it is necessary to analytically determine the error in the estimate of the absorption coefficient that is calculated employing this assumption, in order to minimize it in the measurements. The absorption coefficient is determined by exposing the tissue to ultrasound and making temperature measurements with embedded thermocouples to evaluate $\partial T_{nc}/\partial t$. The measurements are performed in a large isotonic saline bath that serves as the uniform-temperature, acoustic coupling medium.[10]

The subscript on T_{nc} indicates that the derivative of the measured temperature increase resulting from ultrasonic exposure is to be evaluated when heat conduction is negligible. In the TTM the derivative is evaluated at small times such that the effect of heat conduction on the measured temperature increase data can be neglected. The temperature derivative is determined indirectly in the PDM by assuming an analytical form for the temperature decay resulting from a short ultrasound pulse and fitting the measured data to the assumed analytical expression. The curve fit then yields $\partial T_{nc}/\partial t$ (Ref. 5). Each technique has advantages and limitations. The existence of an error in evaluating the derivative of the temperature, which arises from viscous heating due to the relative motion of the embedded thermocouple and the tissue, is well known.[7,11] The TTM attempts to minimize this artifact by evaluating the temperature derivative at a time sufficiently long such that the contribution of the viscous heating to the derivative is negligible. This necessitates using small thermocouples and large acoustic beamwidths to provide a temporal window during which the viscous artifact is minimal, while heat conduction is still negligible. The PDM avoids having to determine this temporal window in estimating the temperature derivative for those situations in which assumptions concerning the acoustic beam profile, tissue boundaries, and homogeneity of the heat conducting medium are met experimentally. Although infinite transverse tissue dimensions are assumed for the PDM as it is currently applied, finite dimensions for rectangular and cylindrical tissue boundaries can be included in the analytical expressions for heat conduction, when heating with a Gaussian transverse beam profile. The PDM is, however, more difficult to implement than the TTM. Thus, for those frequencies and beamwidths for which the accuracy of the two methods is comparable, the TTM may be a more desirable technique.

A difference in reported values of absorption between the PDM and TTM has indicated a need for analysis and improvement in the measurement techniques.[12] Specifically, absorption coefficient measurements reported on liver employing the PDM were 14% higher than those employing the TTM at low megahertz frequenices, with greater differ-

 0001-4966/90/080967-11$00.80

ences at higher frequencies. A theoretical and experimental investigation of absorption coefficient measurements using the PDM has been reported.[12,13] Error estimates were presented and guidelines were given for making accurate estimates of the absorption coefficient with this technique. However, no comparable study of the TTM has been reported. The primary sources of error in applying the TTM to determine the absorption coefficient is heat conduction toward or away from the temperature sensor and the viscous heating artifact associated with the temperature sensor. A previous study of the heat-conduction error resulting from the finite transverse half-power beamwidth (HPBW) of the acoustic beam, and the viscous heating artifact due to the presence of the embedded thermocouple, yielded guidelines for selecting the most appropriate size of thermocouple and specifications of the HPBW when applying the TTM.[11] The modeling of acoustic wave propagation, however, did not account for attenuation of the plane wave propagating in the tissue, and heat conduction to the tissue-coupling medium boundary was not investigated. In addition, the time derivative of the temperature was evaluated only at 0.5 s.[11]

The purpose of the present study is to quantify theoretically the errors resulting from heat conduction for a prescribed acoustic beamwidth and specified tissue dimensions, when using the TTM to measure the ultrasonic absorption coefficient in soft tissue. Experimental guidelines for minimizing errors due to finite beamwidth and tissue dimensions, absorption, and viscous heating result from the analysis. An expression is defined for the relative error at any given time after the initiation of a unit-step ultrasonic pulse. The relative error is the difference between the results obtained in the ideal situation with no heat conduction as represented by Eq. (1) and the results obtained using the model of the experimental situation, which includes heat conduction due to finite beamwidths, finite tissue dimensions, and absorption. Results are presented for various beamwidths, specimen dimensions, and absorption coefficients. The analysis provides fundamental limits on the accuracy of a measurement of the absorption coefficient employing the TTM within the limitations of the model. For example, measurements of the absorption coefficient for tissues of small dimensions have been reported[14,15] where uncertainties concerning the accuracy of the measurement remain because of the effect of heat conduction on the temperature derivative at the time of evaluation. The results presented herein provide the fundamental limit imposed by finite beamwidth and sample dimensions on the accuracy of such measurements. A further example of the utility of the analysis presented herein is in reducing the error introduced in the derivative of the temperature by the viscous heating from the presence of the thermocouple. As the TTM is currently applied in the Bioacoustics Research Laboratory, and in the original papers by Fry and Fry,[7,8] it is prescribed that the time derivative of the temperature is to be evaluated at 0.5 s following the initiation of a unit step ultrasonic exposure. However, for sufficiently large tissue dimensions and beamwidths, as shown in Sec. II, the time derivative of the temperature can be evaluated at times later than 0.5 s without significantly increasing the error due to heat conduction, while decreasing the error resulting from the viscous heating artifact. Finally, by quantifying the error associated with heat conduction that results from finite beam dimensions, the beamwidths for which the PDM can provide greater accuracy are determined. The narrowing of the acoustic beam for single, focused radiators is particularly important at higher frequencies.

The thermal properties of the tissue and water coupling medium are assumed uniform as in previous studies.[5,6,11] The use of this model for the thermal properties of the water–tissue medium has been verified by previous experiments.[5,6,11,12,16] A focused acoustic field is modeled as a circularly symmetric Gaussian beam,[5,17] and includes plane-wave attenuation in the tissue. Linear-wave propagation is assumed. Planar boundaries are assumed for the tissue; i.e., the tissue possesses rectangular geometry. The Gaussian beam acoustic profile, together with assumed planar boundaries, allows the temperature for an arbitrary irradiation time envelope to be expressed in terms of a single integral. The error is then defined and investigated as a function of time, acoustic beamwidth, sample dimensions, and absorption.

I. THEORY

A schematic representation of the TTM measurement configuration is shown in Fig. 1. A soft tissue specimen with ultrasonic absorption coefficient α, heat capacity per unit mass C_p, and thermal diffusivity κ is irradiated with a focused ultrasound source. A thermocouple probe of small diameter, embedded at a depth d in the tissue, is the temperature sensor. The tissue is assumed to have planar boundaries with a surface facing the ultrasonic source and oriented normal to the acoustic axis of propagation as shown in Fig. 1. The position vector $\mathbf{r}$ is used to denote the site of temperature observation, relative to the center of the focal region, as determined in the free field. The experimental environment is modeled for heat conduction as an infinite, isotropic, homogeneous medium, with a zero temperature increase at infinity, and zero initial conditions. A diffusion length $l = \sqrt{4\kappa t}$ may be defined that is indicative of the spatial extent of the heating due to a localized heat source at a given time t. For a time of 2 s and a thermal diffusivity characteristic of water, $\kappa = 1.5 \times 10^{-3}$ cm^2/s, the diffusion length is 0.11 cm. The

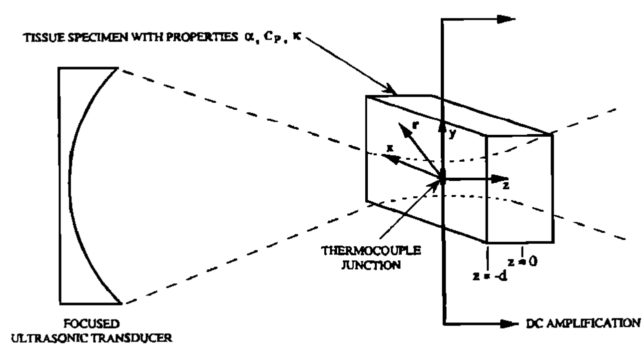

FIG. 1. Schematic representation of the experimental procedure, conducted in a large, isotonic saline bath.

size of the water bath in which the absorption coefficient measurements are performed is typically more than two orders of magnitude greater than this; hence, the medium may be considered infinite. The thermal diffusivity of many soft tissues is approximately that of water,[18] such that the entire medium may be considered homogeneous. Exceptions are skin and fat with thermal diffusivities of approximately 1×10^{-3} cm^2/s.

The temperature $T(\mathbf{r},t)$ at any point of observation $\mathbf{r}$ and time t is then given by the solution of the inhomogeneous heat equation

$$\frac{\partial T}{\partial t} - \kappa \nabla^2 T = Q(\mathbf{r},t). \tag{2}$$

The source term $Q(\mathbf{r},t)$ in Eq. (2) is given by

$$Q(\mathbf{r},t) = Q_0 f(\mathbf{r}) F(t) = (2\alpha/\rho C_p) I(\mathbf{r}) F(t), \tag{3}$$

for a traveling plane wave in an absorptive medium, where $I(\mathbf{r})$ is the intensity as a function of position, and $F(t)$ is the time dependence. The temperature increase resulting from ultrasonic absorption as well as the absolute temperature is governed by the heat equation; however, only the temperature increase is important for present purposes. Thus $T(\mathbf{r},t)$ in Eq. (2) is the temperature increase above the ambient temperature in the bath. A solution to Eq. (2) can be obtained for the assumed model by the method of Green's functions. The temperature at position $\mathbf{r}$ and time t is given by

$$T(\mathbf{r},t) = Q_0 \int_0^t d\tau\, F(\tau) \int_V d\mathbf{r}'\, f(\mathbf{r}') G(\mathbf{r}-\mathbf{r}', t-\tau), \tag{4}$$

where

$$G(\mathbf{r}-\mathbf{r}', t-\tau) = \frac{\exp[-|\mathbf{r}-\mathbf{r}'|^2/4\kappa(t-\tau)]}{[4\pi\kappa(t-\tau)]^{3/2}}$$

is the Green's function for an infinite, isotropic, homogeneous medium, and the volume integration is performed over the region of the absorbing soft tissue.[19]

The linear, focused acoustic beam is modeled with a Gaussian dependence in both the transverse and axial directions. The error for a Gaussian beam is compared to a $[2J_1(ar)/ar]^2$ [henceforth referred to as uniform displacement, circular aperture (UDCA)] beam shape transverse to the direction of propagation in Sec. III. The Gaussian shape in the axial direction has been shown to be a reasonable first-order approximation for medium and highly focused beams in the focal region.[17,20] A piecewise linear approximation to the axial beam variation will also result in an analytical expression for the temperature increase due to absorption; however, a Gaussian shape is adequate for a first-order approximation. The shape of the theoretical transverse profile for a focused, cylindrically symmetric radiator at the center of the radius of curvature, as well as the transverse profile for an unfocused radiator in the farfield, is given by a UDCA profile. Although the axial variation of the beam radiated by a planar source differs considerably from a Gaussian function over the entire field, a Gaussian shape is still a useful approximation at the near-field–far-field transition region, for dimensions typically of concern in the TTM. Hence, the analysis presented is useful for unfocused as well as for focused sources.

The intensity distribution in a dissipationless medium is taken to be

$$I(\mathbf{r}) = I(r,z) = I_0 \exp(-r^2/\beta_r - z^2/\beta_z), \tag{5}$$

where $r^2 = x^2 + y^2$, β_r and β_z are the beamwidth parameters in the transverse and axial dimensions, respectively, and I_0 is the spatial peak intensity at $(r,z) = (0,0)$. The beamwidth parameters β_r and β_z are related to the radial and axial HPBWs by $\beta_i = (\frac{1}{2}\mathrm{HPBW})^2/\ln 2$, where i denotes either the radial or axial dimension. The axial half-power beamwidth, which for clarity will be referred to as the half-power beamlength (HPBL), is approximately ten times greater than the radial HPBW for medium and highly focused beams, and a factor of 10 will be used in the analysis.[10] The intensity distribution for a traveling plane wave in a tissue specimen with absorption coefficient α and boundary through which the ultrasound enters at $z = -d$ is considered to be

$$I(\mathbf{r}) = I(r,z) = I_0 \exp[-2\alpha(z+d)] \exp(-r^2/\beta_r - z^2/\beta_z). \tag{6}$$

The exponential decay in the intensity is assumed to result primarily from absorption.[9] In using the functional form of Eq. (5) multiplied by a decaying exponential term as the intensity distribution in the tissue, as given in Eq. (6), it has been assumed that propagation in the tissue does not significantly affect the shape of the acoustic beam. This assumption may be somewhat tenuous for very thick specimens,[9] although the results will show that only the intensity distribution over a few millimeters into the tissue is of consequence. Substituting the Gaussian beam shape of Eq. (6) into Eq. (4), and introducing the limits of integration for the planar boundaries, the temperature increase is given by

$$T(\mathbf{r},t) = \frac{2\alpha I_0}{\rho C_p} \int_0^t d\tau\, F(\tau) \int_{-d}^{z_2} dz' \int_{-y_1}^{y_2} dy' \int_{-x_1}^{x_2} dx' \exp[-2\alpha(z'+d)] \exp\left(-\frac{x'^2+y'^2}{\beta_r} - \frac{z'^2}{\beta_z}\right)$$
$$\times \exp\left[-\left(\frac{(x-x')^2 + (y-y')^2 + (z-z')^2}{4\kappa(t-\tau)}\right)\right] \{[4\pi\kappa(t-\tau)]^{3/2}\}^{-1}. \tag{7}$$

After performing the volume integration, the temperature increase at any point $\mathbf{r} = (x,y,z)$ and time t is given by

$$T(\mathbf{r},t) = (2\alpha I_0/\rho C_p) e^{-2\alpha d} v(\mathbf{r},t,\beta_r,\beta_z,\alpha), \tag{8}$$

where

$$v(\mathbf{r},t,\beta_r,\beta_z,\alpha) = \int_0^t d\tau\, F(\tau)\exp\left[-\left(\frac{r^2}{\beta_r}\frac{1}{1+4\kappa(t-\tau)/\beta_r}\right)\right]\left(1+\frac{4\kappa(t-\tau)}{\beta_r}\right)^{-1}$$
$$\times\exp\left[-\left(\frac{z^2}{\beta_z}\frac{1}{1+4\kappa(t-\tau)/\beta_z}+\frac{2\alpha z-4\alpha^2\kappa(t-\tau)}{1+4\kappa(t-\tau)/\beta_z}\right)\right]\left[\left(1+\frac{4\kappa(t-\tau)}{\beta_z}\right)^{1/2}\right]^{-1}$$
$$\times\frac{1}{2}\left\{\mathrm{erf}\left[\frac{1}{\sqrt{4\kappa(t-\tau)}}\left(1+\frac{4\kappa(t-\tau)}{\beta_r}\right)^{1/2}\left(\frac{1}{1+4\kappa(t-\tau)/\beta_r}x+x_1\right)\right]\right.$$
$$\left.-\,\mathrm{erf}\left[\frac{1}{\sqrt{4\kappa(t-\tau)}}\left(1+\frac{4\kappa(t-\tau)}{\beta_r}\right)^{1/2}\left(\frac{1}{1+4\kappa(t-\tau)/\beta_r}x-x_2\right)\right]\right\}$$
$$\times\frac{1}{2}\left\{\mathrm{erf}\left[\frac{1}{\sqrt{4\kappa(t-\tau)}}\left(1+\frac{4\kappa(t-\tau)}{\beta_r}\right)^{1/2}\left(\frac{1}{1+4\kappa(t-\tau)/\beta_r}y+y_1\right)\right]\right.$$
$$\left.-\,\mathrm{erf}\left[\frac{1}{\sqrt{4\kappa(t-\tau)}}\left(1+\frac{4\kappa(t-\tau)}{\beta_r}\right)^{1/2}\left(\frac{1}{1+4\kappa(t-\tau)/\beta_r}y-y_2\right)\right]\right\}$$
$$\times\frac{1}{2}\left\{\mathrm{erf}\left[\frac{1}{\sqrt{4\kappa(t-\tau)}}\left(1+\frac{4\kappa(t-\tau)}{\beta_z}\right)^{1/2}\left(\frac{z-4\alpha\kappa(t-\tau)}{1+4\kappa(t-\tau)/\beta_z}+d\right)\right]\right.$$
$$\left.-\,\mathrm{erf}\left[\frac{1}{\sqrt{4\kappa(t-\tau)}}\left(1+\frac{4\kappa(t-\tau)}{\beta_z}\right)^{1/2}\left(\frac{z-4\alpha\kappa(t-\tau)}{1+4\kappa(t-\tau)/\beta_z}-z_2\right)\right]\right\} \quad (9)$$

and erf denotes the error function.

The results for the PDM can be obtained from Eq. (8) by neglecting the exponential decrease of the intensity, letting the boundaries go to infinity, and observing the temperature at $r=0$, yielding[5]

$$T(0,t) = \frac{2\alpha I_0}{\rho C_p}\int_0^t d\tau\, F(\tau)\times\left(1+\frac{4\kappa(t-\tau)}{\beta_r}\right)^{-1}\left[\left(1+\frac{4\kappa(t-\tau)}{\beta_z}\right)^{1/2}\right]^{-1}. \quad (10)$$

By letting $\beta_z\to\infty$, i.e., assuming an axially uniform beam, Eq. (10) can be integrated for a short ultrasonic pulse $F(t)=U(t)-U(t-t_0)$, where $U(t)$ is the unit step function, to yield

$$T(0,t) = \frac{2\alpha I_0}{\rho C_p}\frac{\beta_r}{4\kappa}\left[\ln\left(1-\frac{4\kappa t_0/\beta_r}{1+4\kappa t/\beta_r}\right)^{-1}\right]. \quad (11)$$

Expanding Eq. (11) in a Taylor series and keeping only the leading-order term, the temperature is given by

$$T(0,t) = \frac{2\alpha I_0}{\rho C_p}t_0\frac{1}{1+4\kappa t/\beta_r}, \quad (12)$$

which is the result previously obtained for the PDM assuming a thermally impulsive source, i.e., $F(t)=\delta(t)$ (Ref. 5). As seen from the preceding development, the ultrasound heating source can be considered thermally impulsive if

$$\frac{4\kappa t_0/\beta_r}{1+4\kappa t/\beta_r}\ll 1. \quad (13)$$

The first 1 s of data, following the initiation of the ultrasound pulse, is typically ignored in implementing the PDM, to allow the temperature artifact from the viscous heating of tissue surrounding the embedded thermocouple to become negligible. Then, Eq. (13) is satisfied for experimental purposes if the length of the ultrasound pulse is of the order of 100 ms or less for any HPBW. For example, a 1-mm HPBW, $\kappa=1.5\times10^{-3}$ cm^2/s, $t=1$ s, and $t_0=100$ ms yields

$$\frac{4\kappa t_0/\beta_r}{1+4\kappa t/\beta_r}=0.062.$$

Recent implementations of the PDM have utilized the integral-differential relationship between the impulse and unit step responses for the heat equation, in determining the absorption coefficient.[12,13] In practice, the temperature history is measured for a unit-step exposure and the impulse response obtained by differentiating the measured data. The usefulness of this procedure is in producing sufficient temperature increases that can be accurately measured, without generating significant harmonic components in the acoustic field, due to nonlinear propagation. A lesser intensity can be used, to produce a measurable temperature increase, with a unit-step ultrasonic exposure than with a short-pulse exposure approximating a delta function.

The error in measuring the absorption coefficient using the TTM, which results from heat conduction due to the finite acoustic beam and tissue boundaries, can be investigated by defining the relative error

$$E(\mathbf{r},t,\beta_r,\beta_z,\alpha) = \left[\left(\frac{\partial T_{nc}}{\partial t}-\frac{\partial T(\mathbf{r},t)}{\partial t}\right)\Big/\frac{\partial T_{nc}}{\partial t}\right]\times 100\%, \quad (14)$$

where T_{nc} is the temperature increase in the absence of heat conduction as given by Eq. (1) and $T(\mathbf{r},t)$ includes heat conduction and is given by Eq. (8) with $F(t)=U(t)$ [in Eq.

[(9)]. Equations (1) and (8) can be used to simplify Eq. (14) to yield

$$E(\mathbf{r},t,\beta_r,\beta_z,\alpha) = \left(1 - \frac{\partial v}{\partial t}\right) \times 100\%. \tag{15}$$

The limits on E as t goes to zero and infinity can be found by using the relation between the impulse and unit step responses for $\partial v/\partial t$ (Ref. 21). In the case of a half-space with the water–tissue interface at $z = -d$, $\partial v/\partial t$ is given by

$$\frac{\partial v}{\partial t} = \exp\left[-\left(\frac{r^2}{\beta_r}\frac{1}{1+4\kappa t/\beta_r}\right)\right]\left(1+\frac{4\kappa t}{\beta_r}\right)\times\exp\left[-\left(\frac{z^2}{\beta_z}\frac{1}{1+4\kappa t/\beta_z}+\frac{2\alpha z-4\alpha^2\kappa t}{1+4\kappa t/\beta_z}\right)\right]\left(1+\frac{4\kappa t}{\beta_z}\right)^{1/2} \times\frac{1}{2}\left\{\operatorname{erf}\left[\frac{1}{\sqrt{4\kappa t}}\left(1+\frac{4\kappa t}{\beta_z}\right)^{1/2}\left(\frac{z-4\alpha\kappa t}{1+4\kappa t/\beta_z}+d\right)\right]+1\right\}. \tag{16}$$

The limits on E as $t \to 0$ and $t \to \infty$ are then

$$\lim_{t\to 0} E = \left[1 - \frac{1}{2}\exp\left(-\frac{r^2}{\beta_r}-\frac{z^2}{\beta_z}-2\alpha z\right) \times \lim_{t\to 0}\left\{\operatorname{erf}\left[\frac{1}{\sqrt{4\kappa t}}\left(1+\frac{4\kappa t}{\beta_z}\right)^{1/2} \times\left(\frac{z-4\alpha\kappa t}{1+4\kappa t/\beta_z}+d\right)\right]+1\right\}\right]\times 100\% \tag{17}$$

and

$$\lim_{t\to\infty} E = 100\%. \tag{18}$$

At the water–tissue interface, the limit on the error function in Eq. (17) goes to zero, and

$$\lim_{t\to 0} E = \left[1 - \frac{1}{2}\exp\left(-\frac{r^2}{\beta_r}-\frac{d^2}{\beta_z}+2\alpha d\right)\right]\times 100\%.$$

For $z < -d$, the relative error in Eq. (17) goes rapidly to 100% as z decreases, and for $z > -d$, E goes rapidly to

$$\left[1 - \exp\left(-\frac{r^2}{\beta_r}-\frac{z^2}{\beta_z}-2\alpha z\right)\right]\times 100\%,$$

as $t \to 0$.

The infinite, isotropic, homogeneous modeling of the thermal properties of the water–tissue medium assumed in the derivation of Eq. (8) neglected heat conduction along the thermocouple wire and loss of heat due to convection at the water–tissue interface. The additional heat conduction due to conduction along the thermocouple wire and to convective loss at the water–tissue interface will result in a lower measured temperature increase in the tissue at the focal point of the ultrasonic beam than predicted by Eq. (8). An increase in the relative error defined in Eq. (14) will result from these additional components of heat conduction away from the thermocouple junction.

II. RESULTS AND DISCUSSION

The integral-differential relation between the impulse and unit step responses can be used to determine $\partial v/\partial t$ without performing the time integration. The error expression of Eq. (14) can then be evaluated as a function of spatial coordinates, time, beamwidth, beamlength, tissue specimen dimensions, and absorption. For the results presented in this section, the axial HPBL is assumed to be ten times the radial HPBW, i.e., $\beta_z = 100\beta_r$ (Refs. 5, 6, 10). The relative error for a Gaussian beam profile as given by Eq. (5) for an infinite heating region is compared with measured results in mouse and horse liver from Goss *et al.* and beef liver from Parker in Fig. 2.[5,11] Since the reported values of the absorption coefficient in liver vary from 0.023 cm^{-1} to greater than 0.04 cm^{-1} at 1 MHz (Refs. 5 and 22), the data from both references are normalized such that the experimental point corresponding to the largest experimental HPBW in both cases falls on the computed error curve. As can be seen, the analytical results compare favorably with the experiments.

The effect of the HPBW on the relative error is shown in Fig. 3 at $t = 0.5$, 1.0, and 1.5 s. The heating volume has been taken to be infinite, and the exponential decay of the intensity in the tissue neglected; hence, the intensity distribution of Eq. (5) is used. The site of temperature observation is $(x,y,z) = (0,0,0)$. As expected, the relative error goes to zero at each of the times shown as the HPBW approaches infinity. For a typical experimental procedure employing a medium-focused acoustic beam with a 5-mm HPBW, the relative error is 3.2%, 6.3%, and 9.1%, at 0.5, 1.0, and 1.5 s,

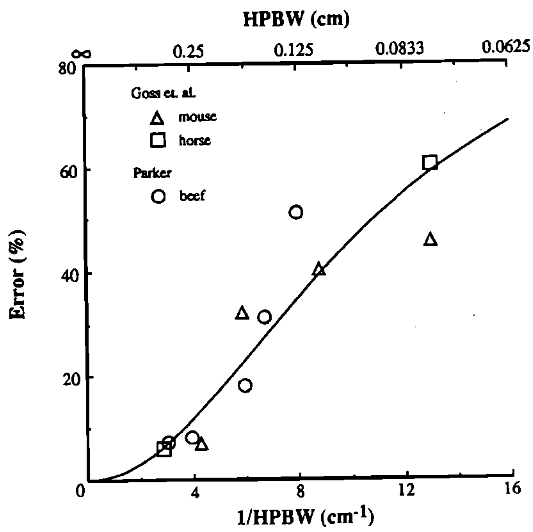

FIG. 2. The relative error versus reciprocal HPBW and HPBW at 0.5 s following initiation of ultrasonic exposure. Comparison of a Gaussian profile (solid line) and experimental results in liver from Goss *et al.* and Parker (symbols).[5,11]

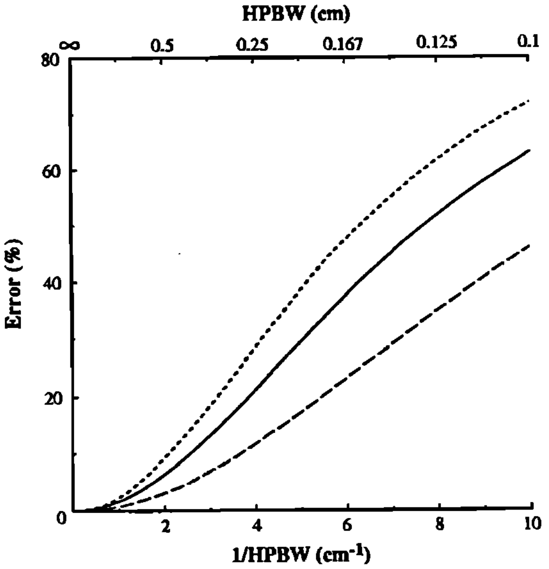

FIG. 3. Relative error versus reciprocal HPBW and HPBW for an absorbing volume of infinite extent at 0.5 (long dashed line), 1.0 (solid), and 1.5 (short dash) s following the initiation of exposure.

respectively. The coefficient of variation (standard deviation expressed as a percentage of the mean) for absorption coefficient measurements using the TTM typically ranges from 10%–30%.[22] Although the defined relative error, which results from heat conduction, can generally be kept smaller than the standard deviation of the measurements, in some instances, the errors resulting from heat conduction can add a significant bias to the estimate. For example, a 1.5-mm HPBW acoustic field will result in an estimate for the absorption coefficient that is greater than 20% too low, or a thermocouple junction at a depth of only 0.5 mm will bias the estimate by more than 10% too low. Heat conduction along the thermocouple also biases the measurement, but for typical experimental procedures employing 13–25-μm constantan–chromel thermocouples, this bias can be made less than 0.5%.[7,23] It has been the practice in the Bioacoustics Research Laboratory to attempt to minimize the error due to heat conduction by employing large acoustic HPBWs and evaluating the time derivative of the temperature at 0.5 s. However, for those experimental situations for which the thermal model used herein is appropriate, e.g., a thermally homogeneous tissue such as liver, the analysis may be used to correct for heat conduction.

It is advantageous to heat for a time longer than 0.5 s before evaluating the derivative $\partial T/\partial t$ for low-absorbing tissues, in order to minimize the error from the viscous heating associated with the thermocouple in the estimate of the absorption coefficient. For a tissue specimen of sufficient dimension that no significant heat flow has occurred due to finite boundaries, at 1 or 1.5 s, a wider HPBW can result in the same percent error at 1.5 s as with a narrow HPBW at 0.5 s. For example, $E = 3.2\%$ at 0.5 s for an HPBW of 5 mm, while $E = 2.5\%$ at 1.5 s for an HPBW of 1 cm. If the heat distribution resulting from the viscous heating is approximated transverse to the wire as a uniform cylinder with a radius equal to that of the thermocouple wire diameter, and along the wire axis as a Gaussian function, with a half-width equal to the acoustic HPBW, the time derivative of this portion of the total temperature increase is given by

$$\frac{\partial T_v}{\partial t} = \frac{q_0 I}{\rho C_p}\,(1 - e^{-r_w^2/4\kappa t})\,\frac{1}{(1 + 4\kappa t/\beta_r)^{1/2}}, \qquad (19)$$

where r_w is the wire radius, and $q_0 I$ is the heat generation rate per unit volume. The heat source is assumed to be in an infinite, isotropic, homogeneous medium with $\kappa = 1.5 \times 10^{-3}$ cm^2/s. Taking the ratio of Eq. (19) and the derivative of Eq. (10) yields an approximation to the error introduced in the measured temperature increase by the presence of the thermocouple. For low-absorbing tissues such as testis, which has an absorption coefficient of 0.017 cm^{-1} at 1 MHz (Ref. 16), the ratio $q_0/2\alpha$ can be large. However, by evaluating the temperature derivative at longer times, the error due to viscous heating can be significantly reduced. For example, employing a thermocouple with a 13-μm diameter, and taking $q_0/2\alpha = 1700$ (Ref. 7), the error in the estimate of the absorption coefficient can be reduced from 24% to 8% by evaluating the temperature derivative at 1.5 s as opposed to 0.5 s.

Although the absorbing volume for the relative error shown in Fig. 3 is infinite, the same conclusion can be reached even for very small absorbing volumes. The relative error versus reciprocal HPBW is shown at 0.5, 1.0, and 1.5 s in Fig. 4 for the Gaussian heating distribution given in Eq. (5) integrated over a cube of dimension $3 \times 3 \times 3$ mm^3. The relative error for a 5-mm HPBW at 0.5 s is 3.2%, while the relative error for a 1-cm HPBW at 1.0 s is 3.4%. It is seen by comparing Figs. 3 and 4 that as the HPBW becomes smaller, the heat conduction at the boundary is small compared to heat conduction resulting from the small HPBW for the times shown.

The relative error as a function of time for several values of tissue thickness and HPBWs is shown in Fig. 5. The site of

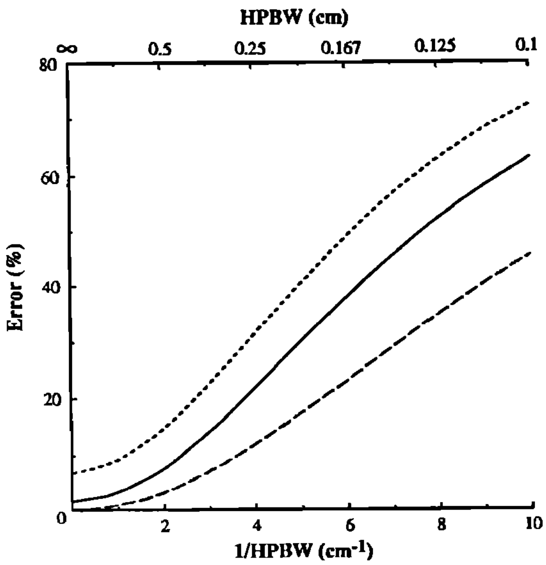

FIG. 4. Relative error versus reciprocal HPBW and HPBW for a $3 \times 3 \times 3$-mm^3 absorbing cube in an infinite medium at 0.5 (long dashed line), 1.0 (solid), and 1.5 (short dash) s following initiation of ultrasonic exposure.

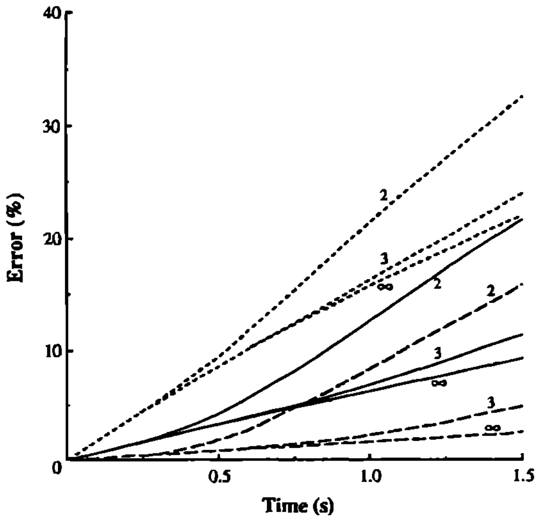

FIG. 5. Relative error versus exposure time for 2, 3, and ∞ mm thicknesses of the absorbing medium at HPBWs of 3 (short dashed lines), 5 (solid), and 10 (long dash) mm.

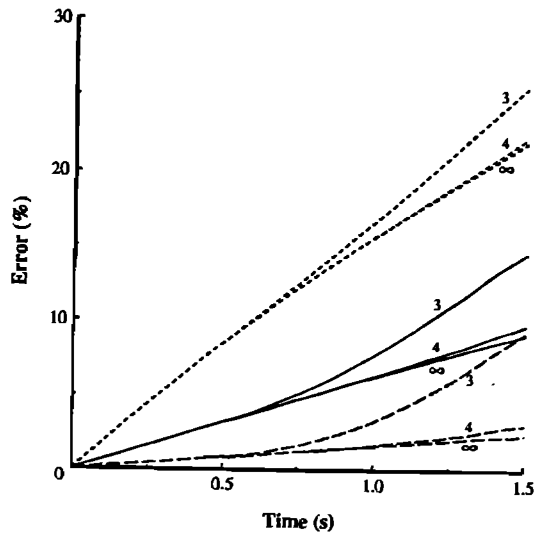

FIG. 6. Relative error versus exposure time for $3\times3\times3$ mm^3, $4\times4\times4$ mm^3, and infinite volumes of absorbing media for 3- (short dashed lines), 5- (solid), and 10- (long dash) mm HPBWs.

temperature observation is taken to be at the center of the specimen thickness. The dimensions transverse to the acoustic axis of propagation, i.e., the x and y directions, are taken to be infinite, and a Gaussian heating distribution as given in Eq. (5) has been assumed. At 0.5 s there is negligible difference between the finite and infinite specimen thicknesses. The contribution of the finite beamwidth to the relative error is more significant (at 0.5 s) than that from the finite size of the tissue specimen. At longer times the portion of the relative error due to the finite sample size becomes very significant. For example, see the 2-mm specimen thickness results. However, a wide HPBW of 1 cm results in a relative error of approximately 5% at 1.5 s even for a 3-mm-thick specimen.

There are experimental situations when it is necessary to measure the absorption coefficient of tissue specimens with dimensions of only a few millimeters.[14,15] The relative error as a function of time for several sizes of cubes, and several values of HPBW, is shown in Fig. 6. The Gaussian function of Eq. (5) has been employed for the heating distribution, and the site of temperature observation is the center of the cube for the finite-dimensional cases and the origin for the infinite-dimensional case. The relative error at 0.5 s for a $3\times3\times3$-mm^3 cube is essentially identical to that for an infinite heating volume. The relative error for a wider HPBW of 1 cm at 1.0 s is 3.4% for a $3\times3\times3$-mm^3 cube and is less than 3.2% for a $4\times4\times4$-mm^3 cube even at 1.5 s. It is clear that the TTM can be employed to measure the absorption coefficient of tissue specimens of small dimensions. The PDM, however, may not be useful in such cases because the tissue boundaries will have an effect on the measured temperature increase. It is then necessary to consider the tissue boundaries in deriving an analytical form for the temperature. The shape of small tissue specimens may not lend themselves easily to boundaries for which an analytical form for the temperature can be found, in particular, rectangular or cylindrical geometries. Thus a significant error may result in using such assumptions in the determination of the absorption coefficient using the PDM.

The relative error at 0.5 s as a function of the thermocouple depth for several values of absorption, α, and a 5-mm HPBW is shown in Fig. 7, for the heating distribution of Eq. (6) over the half-space $z > -d$. The site of temperature observation is the origin, and the beginning of the half-space is the depth. The relative error does not exhibit a rapid increase for increasing thermocouple depth as might be expected for the case of $\alpha \neq 0$, because in the ideal case of negligible heat conduction given by Eq. (1), the exponential decay of the intensity is assumed. Hence, the $e^{-2\alpha d}$ factor in Eq. (8) has been normalized from the expression for E. The z dependence of $\partial v/\partial t$ at 0.5 s, as given by Eq. (16), then causes E to be less in the absorbing, than in the nonabsorbing case, at depths for which the boundary has no effect. Physically, for

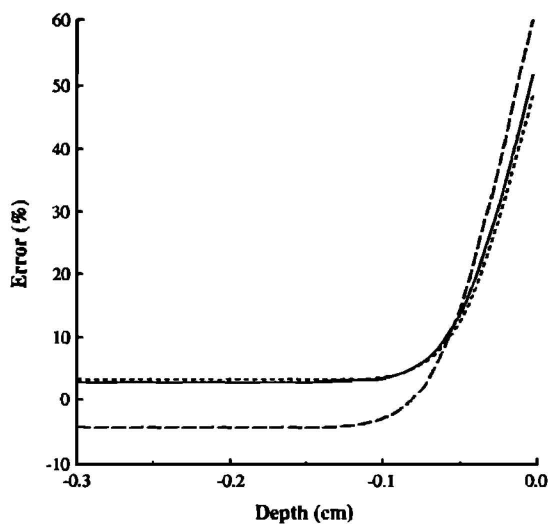

FIG. 7. Relative error versus depth of observation for an absorbing half-space with a Gaussian heating distribution exponentially decaying from the interface for $\alpha = 0$ (short dashed line), $\alpha = 1.0$ (solid), and $\alpha = 5.0$ (long dash), error at 0.5 s for a 5-mm HPBW.

large absorption coefficients, the observation point at $z=0$ is on the tail of a heat distribution exponentially decreasing with depth. Hence, the temperature increase with time, at $z=0$, results from absorption, and heat flow from the region $-d<z<0$. As a result, the relative error can even be negative upon normalizing the $e^{-2\alpha d}$ factor from the expression for E. The absorption is important in contributing to the error if the depth at which the thermocouple is placed is not precisely known. The assumption in arriving at Eq. (8) has been that the embedded thermocouple is located at the beam maximum, i.e., $z=0$, as determined in the free field, and that the depth in the tissue at which the junction is located is precisely known. As seen in Eq. (16), $\partial v/\partial t$ has an $\exp\{-[2\alpha z/(1+4\kappa t/\beta_z)]\}$ dependence, where $z>-d$ is the location of the thermocouple junction. Essentially, this factor represents an error in the calculated intensity resulting from the error in the position. This factor becomes particularly important at higher frequencies where the absorption coefficient is larger. For example, at 8 MHz the absorption coefficient for liver is approximately 0.5 cm^{-1} (Ref. 12). For an HPBW of 5 mm, an absorption coefficient of 0. 5 cm^{-1}, and a positioning error of 1 mm, i.e., $z=+1$ mm, the above exponential factor contributes 9% to the error at 0.5 s following the initiation of exposure. The exponential factor $\exp\{-(z^2/\beta_z)[1/(1+4\kappa t/\beta_z)]\}$ in $\partial v/\partial t$ contributes negligibly to this error for the given values of HPBW and z.

The relative error as a function of thermocouple depth in the tissue at 0.5, 1.0, and 1.5 s, with $\alpha=0$, is shown in Fig. 8(a) and (b) for 5-mm and 1-cm HPBWs, respectively. At $t=0.5$ s, no significant heat conduction results from the half-space boundary for thermocouples placed 1 mm or deeper in both cases. The asymptotic value of the error with increasing depth is determined by the beamwidth as can be seen by comparing Fig. 8(a) and (b) with the appropriate HPBWs in Fig. 3. Defining a critical depth as the depth at which heat conduction toward the boundary is negligible, at $t=0.5$, 1.0, and 1.5 s, the critical depth is approximately 1.0, 1.5, and 1.75 mm, respectively. It is advantageous to place the thermocouple deeper than the critical depth because of the rapid rise in the relative error for more shallow depths, as is seen in Fig. 8(a) and (b).

The thermocouple junction is centered on the acoustic beam when measuring the absorption coefficient using the TTM. The center of the beam is found by stepping the thermocouple junction transversely across the beam and recording the temperature increase that results from a short ultrasonic pulse. The resulting set of points is then fit to a second- or fourth-order polynomial and the thermocouple junction positioned at the maximum of the fitted curve. Errors in finding the beam maximum by this procedure can result from noise and from sampling increments that are too large. The relative error as a function of time for 3- and 5-mm HPBWs for several displacements from the beam maximum is shown in Fig. 9(a) and (b), computed using the Gaussian heating distribution of Eq. (5) over an infinite absorbing region. As with an axial error in the estimate of the position, a radial positioning error essentially results in an error in the estimate of the intensity for the times of interest. In general, the thermocouple junction can be precisely positioned at the center of the acoustic beam profile. Figure 9(a) and (b) emphasizes that precision is necessary in finding the beam maximum for narrow HPBWs.

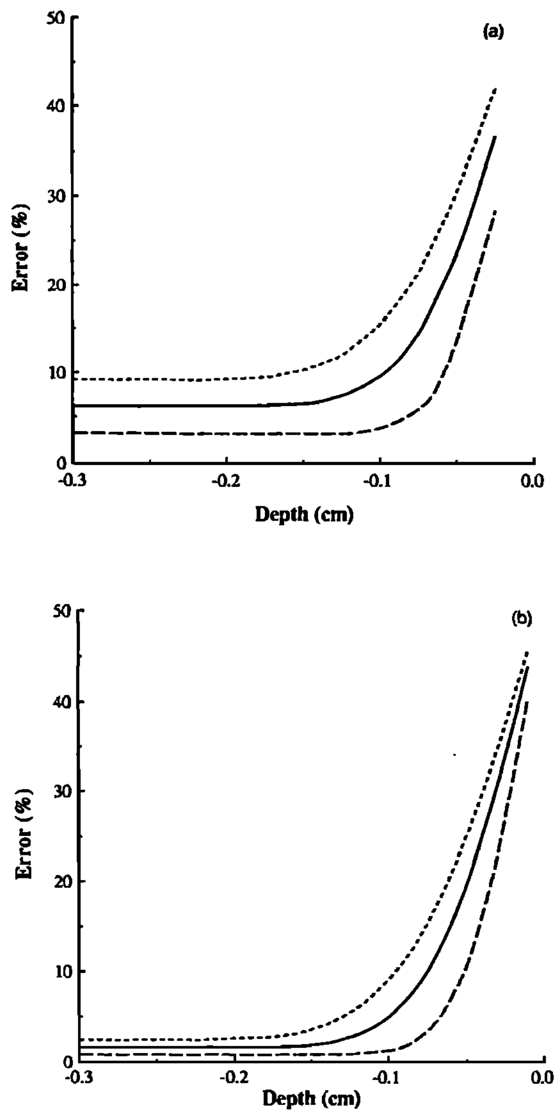

FIG. 8. Relative error versus depth of observation for an absorbing half-space for a Gaussian heating distribution and no exponential decay for (a) a 5-mm HPBW at 0.5 (long dashed line), 1.0 (solid), and 1.5 (short dash) s following the initiation of exposure; (b) same as (a) with a 1-cm HPBW.

III. COMPARISON OF GAUSSIAN AND UDCA BEAMS

A Gaussian approximation to the theoretical UDCA intensity profile for a focused radiator at the focal point has been employed in Sec. I. This approximation resulted in a simple analytical expression for $\partial T/\partial t$ for a rectangular absorbing region. The ease in handling the Gaussian approximation analytically makes it more desirable to use for the intensity profile of a focused transducer than the UDCA profile. However, to use the results for the Gaussian beam approximation presented in Sec. II directly, it is first necessary to compare the relative error for a Gaussian beam to that for a real focused radiator. The relative error between

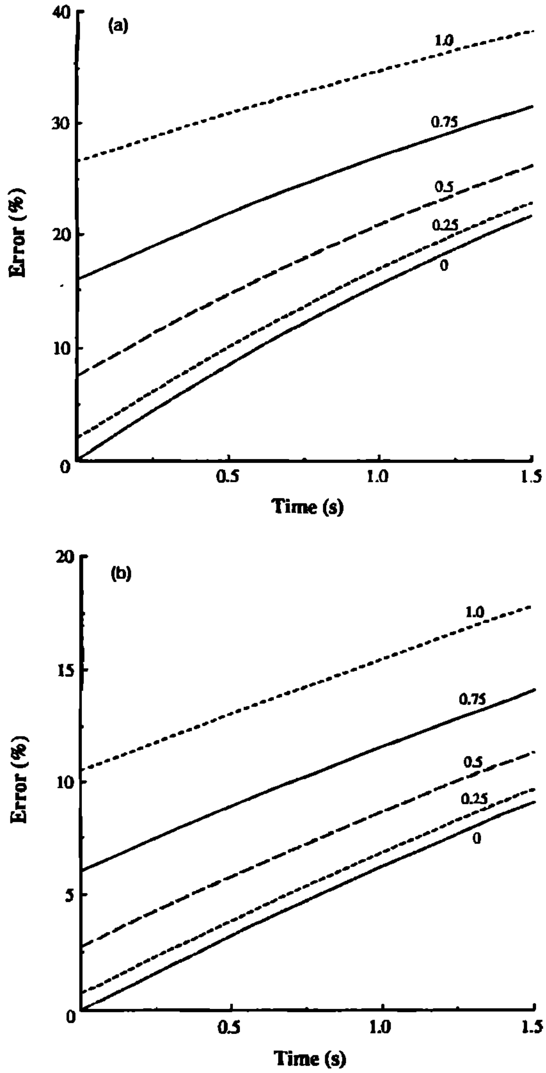

FIG. 9. Relative error versus exposure time for observation points displaced radially (in mm) from the acoustic beam maximum for (a) 3-mm and (b) 5-mm HPBWs.

the cases of no heat conduction and heat conduction for each heat distribution is defined as in Sec. I. The relative error for a circularly symmetric, axially uniform beam in an infinite, thermally homogeneous and isotropic medium can be compared for Gaussian and UDCA beams by solving Eq. (2) with the appropriate source functions. In this case the ultrasound beam is considered to heat the entire region. Equation (2) is again solved by the Green's function method. The temperature as a function of the radial coordinate r, and time t, for a heat distribution $Q(\mathbf{r},t) = Q_0F(t)f(\mathbf{r})$ is given by

$$T(r,t) = Q_0 \int_0^t F(\tau)d\tau \int_0^\infty r'\,dr'\,f(r')G(r,r',t-\tau), \tag{20}$$

where

$$G(r,r',t-\tau) = \frac{\exp[-(r^2+r'^2)/4\kappa(t-\tau)]}{2\kappa(t-\tau)} I_0\left(\frac{rr'}{2\kappa(t-\tau)}\right)$$

is the two-dimensional cylindrically symmetric Green's function, and I_0 is the modified Bessel function of order zero. The difference in the relative error is given by

$$\delta E = |E_J - E_G| = \left|\frac{\partial v_J}{\partial t} - \frac{\partial v_G}{\partial t}\right| \times 100\%, \tag{21}$$

where the J and G subscripts indicate the temperature distribution is to be solved with the UDCA and Gaussian intensity profiles, respectively. Using the integral-differential relation between the impulse and unit step responses, the derivatives $\partial v_J/\partial t$ and $\partial v_G/\partial t$ for $F(t) = U(t)$ are then

$$\frac{\partial v_J(r,t)}{\partial t} = \int_0^\infty r'\,dr' \left(\frac{2J_1(ar')}{ar'}\right)^2 \times \frac{\exp[-(r^2+r'^2)/4\kappa t]}{2\kappa t} I_0\left(\frac{rr'}{2\kappa t}\right), \tag{22}$$

and

$$\frac{\partial v_G(r,t)}{\partial t} = \int_0^\infty r'\,dr' \exp\left(-\frac{r'^2}{\beta_r}\right) \times \frac{\exp[-(r^2+r'^2)/4\kappa t]}{2\kappa t} I_0\left(\frac{rr'}{2\kappa t}\right), \tag{23}$$

where a and β_r are the beam parameters for UDCA and the Gaussian profiles, respectively. By making the temperature observation at the origin, i.e., $r = 0$, the Gaussian function can be integrated analytically to yield

$$\frac{\partial v_G(0,t)}{\partial t} = \frac{1}{1 + 4\kappa t/\beta_r}. \tag{24}$$

The two beam profile functions are compared in Fig. 10 for identical HPBWs of 3 mm. The difference in the relative error $\delta E(t)$ is shown in Fig. 11 for 1-, 3-, 5-, and 10-mm HPBW intensity profiles. The behavior of δE with time is the same in all four curves, with the exception of the time scale, although only the first 2 s following the initiation of the ultrasonic exposure are shown here. The main features of δE as a function of time occur within the first two seconds of expo-

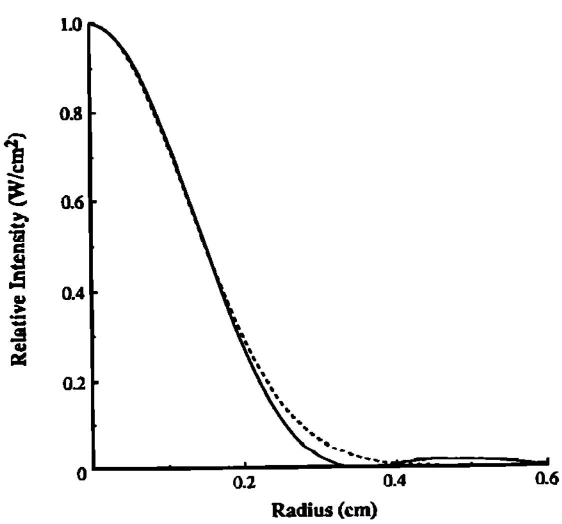

FIG. 10. Comparison of Gaussian (dashed line) and $[2J_1(ar)/ar]^2$ (solid) beams for identical HPBWs of 3 mm.

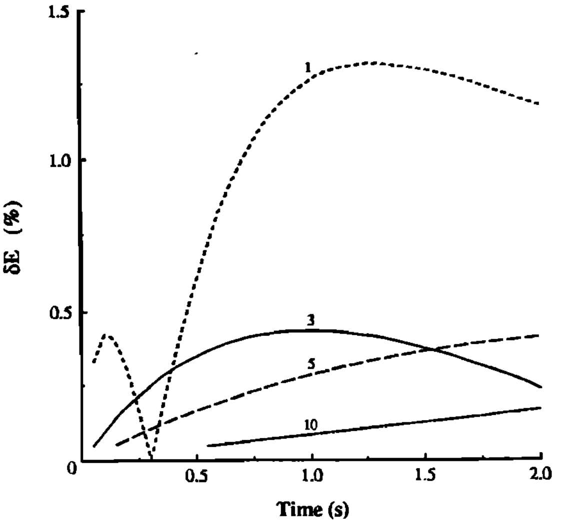

FIG. 11. δE versus exposure time for 1-, 3-, 5-, and 10-mm HPBWs.

sure for a 1-mm HPBW. Initially, $\partial v_J/\partial t > \partial v_G/\partial t$, reaching a maximum of $\delta E = 0.43\%$ at 0.1 s following the initiation of the ultrasonic exposure. The difference in the relative error goes to zero and then increases again with $\partial v_J/\partial t < \partial v_G/\partial t$, reaching a maximum of 1.3%. At longer times, the steady state is approached and $\partial E \to 0$ at $t \to \infty$. The second maximum for the 3-, 5-, and 10-mm HPBWs is not reached in the first 2 s following the initiation of exposure, and $\partial E(t)$ remains less than 0.5% over this time interval. Thus, for beamwidths of concern in using the TTM to measure the ultrasonic absorption coefficient, a Gaussian beam is a good approximation to a UDCA profile for identical HPBWs.

IV. SUMMARY

It is clear that heat conduction can contribute a significant error to the measurement of the ultrasonic absorption coefficient when using the TTM. The temperature increase in a soft tissue specimen irradiated by a traveling plane wave has been derived in this paper for the purpose of evaluating fundamental limits of the TTM and to serve as an experimental guideline for improving the accuracy of the measurement of the ultrasonic absorption coefficient using the TTM. The infinite, isotropic, homogeneous modeling of the heat conducting medium introduced earlier has been employed in this study. The acoustic beam profile has been approximated, transverse to and along the axis of propagation, as Gaussian. A relative error that represents the difference between the case of negligible heat conduction and the assumed model for the experimental environment was defined. The relative error has been studied for varying spatial coordinates, time, radial and axial beamwidth, and absorption.

The analysis demonstrates that HPBWs of the order of 1 cm result in a significantly lesser error than more highly focused beams. A wider HPBW has the advantage that the time derivative of the temperature can be evaluated at times longer than 0.5 s, e.g., 1.0 or 1.5 s, for an error due to heat conduction less than 5% in most practical cases. The contribution of the thermocouple related viscous heating to the temperature derivative is then reduced, thereby improving the estimate of the absorption coefficient. The effect of absorption on the accuracy of the measurement was found to be important only when the actual depth of the thermocouple junction differed from the assumed position, and then was significant only for large absorption coefficients. The depth at which the thermocouple junction should be located, such that heat conduction at the water–tissue interface is negligible, was found to be a function of time. The critical depth at 0.5 and 1.5 s was found to be 1 and 1.75 mm, respectively. Linear-wave propagation was assumed; however, it is possible to extend the analysis to include the error contributed by harmonic absorption in a nonlinear acoustic field to the measurement of the absorption coefficient at a given frequency.[24]

The error in the TTM measurement increases as the frequency is increased because of the decrease in the HPBW of the acoustic beam for single, focused, radiating elements. Larger HPBWs at higher frequencies entail longer focal distances over which nonlinear distortions in the acoustic wave may result. The error in the TTM measurement due to heat conduction can be kept under 10% for HPBWs greater than 3 mm. However, for the narrow HPBWs typically encountered at high frequencies, and at high intensities, the PDM measurement can be expected to yield more accurate results than the TTM.

[1]L. A. Frizzell, C. A. Linke, E. L. Carstensen, and C. W. Fridd, "Thresholds for focal lesions in rabbit kidney, liver, and testicle," IEEE Trans. Biomed. Eng. BE-24, 393–396 (1977).

[2]L. A. Frizzell, "Threshold dosages for damage to mammalian liver by high intensity focused ultrasound," IEEE Trans. Ultrason. Ferroelectr. Freq. Control UFFC-35, 578–581 (1988).

[3]F. J. Fry, G. Kossoff, R. C. Eggleton, and F. Dunn, "Threshold ultrasonic dosages for structural changes in the mammalian brain," J. Acoust. Soc. Am. 48, 1413–1417 (1970).

[4]F. Dunn, P. D. Edmonds, and W. J. Fry, "Absorption and dispersion of ultrasound in biological media," in *Biological Engineering*, edited by H. P. Schwan (McGraw-Hill, New York, 1969), Chap. 3, pp. 205–332.

[5]K. J. Parker, "The thermal pulse decay technique for measuring ultrasonic absorption coefficients," J. Acoust. Soc. Am. 74, 1356–1361 (1983).

[6]K. J. Parker, "Effects of heat conduction and sample size on ultrasonic absorption measurements," J. Acoust. Soc. Am. 77, 719–725 (1985).

[7]W. J. Fry and R. B. Fry, "Determination of absolute sound levels and acoustic absorption coefficients by thermocouple probes—theory," J. Acoust. Soc. Am. 26, 294–310 (1954).

[8]W. J. Fry and R. B. Fry, "Determination of absolute sound levels and acoustic absorption coefficients by thermocouple probes—experiment," J. Acoust. Soc. Am. 26, 311–317 (1954).

[9]K. J. Parker, "Ultrasonic attenuation and absorption in liver tissue," Ultrasound Med. Biol. 9, 363–369 (1983).

[10]W. J. Fry and F. Dunn, "Ultrasound: analysis and experimental methods in biological research," in *Physical Techniques in Biological Research*, edited by W. L. Nastuck (Academic, New York, 1962), Vol. 4, Chap. 6, pp. 261–394.

[11]S. A. Goss, J. W. Cobb, and L. A. Frizzell, "Effect of beam width and thermocouple size on the measurement of ultrasonic absorption using the thermoelectric technique," IEEE Ultrasonics Symp. Proc., 206–211 (1977).

[12]M. E. Lyons and K. J. Parker, "Absorption and attenuation in soft tissues: II—experimental results," IEEE Trans. Ultrason. Ferroelectr. Freq. Control UFFC-35, 511–521 (1988).

[13]K. J. Parker and M. E. Lyons, "Absorption and attenuation in soft tissues: I—calibration and error analyses," IEEE Trans. Ultrason. Ferroelectr. Freq. Control UFFC-35, 242–252 (1988).
[14]K. I. Carnes and F. Dunn, "Absorption of ultrasound by mammalian ovaries," J. Acoust. Soc. Am. 84, 434–437 (1988).
[15]N. B. Smith, T. H. Shepard, and W. D. O'Brien, Jr., "Ultrasonically induced temperature rise in rat embryos," J. Acoust. Soc. Am., 1990, submitted.
[16]S. A. Goss, L. A. Frizzell, and F. Dunn, "Frequency dependence of ultrasonic absorption in mammalian testis," J. Acoust. Soc. Am. 63, 1226–1229 (1978).
[17]P. P. Lele, "A simple method for production of trackless focal lesions with focused ultrasound; physical factors," J. Physiol. 160, 494–511 (1962).
[18]K. M. Sekins and A. F. Emery, "Thermal science for physical medicine," in *Therapeutic Heat and Cold*, edited by J. F. Lehman (Williams and Wilkins, Baltimore, MD, 1982), Chap. 3, pp. 70–132.
[19]N. M. Ozisik, *Heat Conduction* (Wiley, New York, 1980), Chap. 6.
[20]T. C. Robinson and P. P. Lele, "An analysis off lesion development in the brain and plastics by high-intensity focused ultrasound at low-megahertz frequencies," J. Acoust. Soc. Am. 51, 1333–1351 (1969).
[21]I. Stakgold, *Green's Functions and Boundary Value Problems* (Wiley, New York, 1979), Chap. 3.
[22]S. A. Goss, L. A. Frizzell, and F. Dunn, "Ultrasonic absorption and attenuation in mammalian tissues," Ultrasound Med. Biol. 5, 181–186 (1979).
[23]B. S. Singh and A. Dybbs, "Error in temperature measurements due to conduction along the sensor leads," J. Heat Transfer Trans. ASME 98, 491–495 (1976).
[24]E. L. Carstensen, N. D. McKay, D. Dalecki, and T. G. Miur, "Absorption of finite amplitude ultrasound in tissues," Acustica 51, 116–123 (1982).